NASA/TM—2005-213589 AIAA–2005–0541

The Influence of Gravity on Joint Shape for Through-Hole Soldering

Peter M. Struk
Glenn Research Center, Cleveland, Ohio

Richard D. Pettegrew and Robert S. Downs
National Center for Space Exploration Research, Cleveland, Ohio

J. Kevin Watson
Johnson Space Center, Houston, Texas

May 2005

The NASA STI Program Office . . . in Profile

Since its founding, NASA has been dedicated to the advancement of aeronautics and space science. The NASA Scientific and Technical Information (STI) Program Office plays a key part in helping NASA maintain this important role.

The NASA STI Program Office is operated by Langley Research Center, the Lead Center for NASA's scientific and technical information. The NASA STI Program Office provides access to the NASA STI Database, the largest collection of aeronautical and space science STI in the world. The Program Office is also NASA's institutional mechanism for disseminating the results of its research and development activities. These results are published by NASA in the NASA STI Report Series, which includes the following report types:

- TECHNICAL PUBLICATION. Reports of completed research or a major significant phase of research that present the results of NASA programs and include extensive data or theoretical analysis. Includes compilations of significant scientific and technical data and information deemed to be of continuing reference value. NASA's counterpart of peer-reviewed formal professional papers but has less stringent limitations on manuscript length and extent of graphic presentations.

- TECHNICAL MEMORANDUM. Scientific and technical findings that are preliminary or of specialized interest, e.g., quick release reports, working papers, and bibliographies that contain minimal annotation. Does not contain extensive analysis.

- CONTRACTOR REPORT. Scientific and technical findings by NASA-sponsored contractors and grantees.

- CONFERENCE PUBLICATION. Collected papers from scientific and technical conferences, symposia, seminars, or other meetings sponsored or cosponsored by NASA.

- SPECIAL PUBLICATION. Scientific, technical, or historical information from NASA programs, projects, and missions, often concerned with subjects having substantial public interest.

- TECHNICAL TRANSLATION. English-language translations of foreign scientific and technical material pertinent to NASA's mission.

Specialized services that complement the STI Program Office's diverse offerings include creating custom thesauri, building customized databases, organizing and publishing research results . . . even providing videos.

For more information about the NASA STI Program Office, see the following:

- Access the NASA STI Program Home Page at ***http://www.sti.nasa.gov***

- E-mail your question via the Internet to help@sti.nasa.gov

- Fax your question to the NASA Access Help Desk at 301–621–0134

- Telephone the NASA Access Help Desk at 301–621–0390

- Write to:
  NASA Access Help Desk
  NASA Center for AeroSpace Information
  7121 Standard Drive
  Hanover, MD 21076

NASA/TM—2005-213589 AIAA–2005–0541

The Influence of Gravity on Joint Shape for Through-Hole Soldering

Peter M. Struk
Glenn Research Center, Cleveland, Ohio

Richard D. Pettegrew and Robert S. Downs
National Center for Space Exploration Research, Cleveland, Ohio

J. Kevin Watson
Johnson Space Center, Houston, Texas

Prepared for the
43rd Aerospace Sciences Meeting and Exhibit
sponsored by the American Institute of Aeronautics and Astronautics
Reno, Nevada, January 10–13, 2005

National Aeronautics and
Space Administration

Glenn Research Center

May 2005

Acknowledgments

The authors would like to thank the following individuals for their valuable contributions to this project: Greg Fedor, Michael Dobbs, Jack Kolis, Anthony Butina, Michael Conley, Robert Lowe, William O'Hara, Edward Van Cise, Allison Bahnsen, Owen Farmer, Julio Estrada, and the crew of the NASA KC–135 aircraft.

This report is a formal draft or working paper, intended to solicit comments and ideas from a technical peer group.

This report contains preliminary findings, subject to revision as analysis proceeds.

Available from

NASA Center for Aerospace Information
7121 Standard Drive
Hanover, MD 21076

National Technical Information Service
5285 Port Royal Road
Springfield, VA 22100

Available electronically at http://gltrs.grc.nasa.gov

The Influence of Gravity on Joint Shape for Through-Hole Soldering

Peter M. Struk
National Aeronautics and Space Administration
Glenn Research Center
Cleveland, Ohio 44135

Richard D. Pettegrew and Robert S. Downs
National Center for Space Exploration Research
Cleveland, Ohio 44135

J. Kevin Watson
National Aeronautics and Space Administration
Johnson Space Center
Houston, Texas 77058

Abstract

An ongoing research effort on reduced gravity soldering is being conducted jointly by the National Center for Space Exploration Research (NCSER), the NASA Glenn Research Center (GRC), and the NASA Johnson Space Center (JSC). Significant changes in porosity and geometry of plated through-hole (PTH) solder joints are observed in reduced gravity as compared to normal gravity. With regards to geometry, experimental data indicates that through-hole solder joints form asymmetrically in both normal and reduced gravity with respect to the amount of solder on either side of the circuit board. In normal gravity, more solder material is observed below the circuit board compared to the amount above the circuit board where the solder is first added. In reduced gravity, the reverse trend is observed, namely, more solder remains above the circuit card than below. To help understand these results, a new and more magnified view of the joint was incorporated in the experiment (part-way through the testing) which provided both spatially and temporally resolved images of the fillet evolution and solidification during the soldering process. Results from these tests support the hypothesis that there is inadequate time or driving force in reduced gravity for the solder joint mass to equilibrate to complete symmetry from top to bottom before solidification. Equilibration to the joints final shape, which can be confounded by bubble evolution within the joint, appears to be influences by factors in addition to gravity such as solder mass added, solder application technique, the soldering iron, and joint preparation.

I. Introduction

NASA's new vision of space exploration beyond low earth orbit will require changes in how spacecraft designs and operations are viewed. Re-supply opportunities will be extremely limited or non-existent, while constraints on mass and volume will limit the degree to which electronics repairs can be conducted through replacement of complete assemblies or even circuit cards. One solution is to repair at the component level, rather than replace entire circuit cards. This would be a significant step beyond the approach currently used aboard the International Space Station (ISS), where electronic repairs are accomplished by removal and replacement of complete assemblies.

Before component level repair can be embraced as the repair mode for spacecraft avionics, the effects of reduced gravity on the soldering process must be fully characterized. This is particularly important on long duration missions, where the service life of a repaired joint could be an important factor. Several soldering experiments have been conducted onboard the Space Shuttle as "Get Away Special" experiments – operating autonomously in the unpressurized payload bay.[1] The limited results available from these experiments demonstrated dominance of surface tension and increased entrapment of flux. A manual soldering experiment was performed on STS-57 in 1993. Interesting qualitative observations made by the crewmember that performed the test included a

perception that the solder joint fillets were more convex than those experienced when soldering in a normal gravity environment and that the solder alloy appeared to solidify more slowly.

Since 2001, an ongoing research effort to develop an in-depth understanding of the influence of reduced gravity environments on the manual soldering process has been conducted jointly by the NCSER, GRC, and JSC. The low gravity portion of this effort has been conducted on NASA's KC-135 research aircraft using soldering hardware identical to that currently available onboard the ISS. The experiment involves manual soldering by a contingent of test operators including both highly skilled technicians and less skilled individuals to provide a skill mix that might be encountered in space mission crews. Emphasis has been placed on PTH device geometries. For selected joints, a magnified view of the formation of the solder joint was recorded. Post-flight analysis consists of a visual inspection, photography, leg-length measurements of the soldered joints, and video analysis. Subsequently, we cross-sectioned and examined the joints using standard metallographic techniques. From digitized images of the cross-sections, we made porosity measurements in a manner consistent with ASTM Standard E1245-00.[2] We have previously reported findings which indicate significant changes in joint porosity and joint geometry in reduced gravity.[3,4,5] This paper presents some additional data on the effect of gravity level (and other process effects) on the final external geometry of the solder joint. Also, we present several observations regarding the formation of solder joints both in normal and reduced gravity.

II. Experiment Overview

We give only a general description of the experiment here as detailed descriptions are presented elsewhere.[3,4,5] The experimental apparatus provides accommodations for a test operator, who is strapped to a seat, to manually solder on a circuit board in an enclosure. The soldering iron is a Weller® TCP 12P with a PTP7 tip and is the same model as currently flown in the soldering kit aboard the ISS. A PTH configuration (Figure 1) is the geometry of choice. The same circuit board configuration was used throughout the tests; however, two different resistor diameter leads (0.66 mm and 0.78 mm) were used. Prior to soldering, the samples were prepared (e.g. cleanliness, tinning, etc.) according to the NASA standard for electrical connections.[6] However, only some of the boards were demoisturized (by an oven bake) prior to soldering. The non-baked boards would simulate conditions more likely encountered in space-missions. The low-gravity environment was generated aboard NASA's KC-135 research aircraft flying in a parabolic trajectory. The aircraft is capable of flying reduced gravity parabolas where the targeted acceleration levels are near 0-g_e or higher (i.e. partial-gravity parabolas). The symbol g_e is the gravitational acceleration at the Earth's surface. Typical partial-gravity parabolas include "Lunar" and "Martian" parabolas, which target accelerations of 0.16-g_e and 0.38-g_e, respectively. While the acceleration levels experienced during these maneuvers are near the targeted values, variations due to pilot adjustment (e.g. rotation of the aircraft about its center of gravity) and other residual motions do occur (e.g. engine vibrations, weather). The effects of these unsteady disturbances have been discussed in a previous paper.[5]

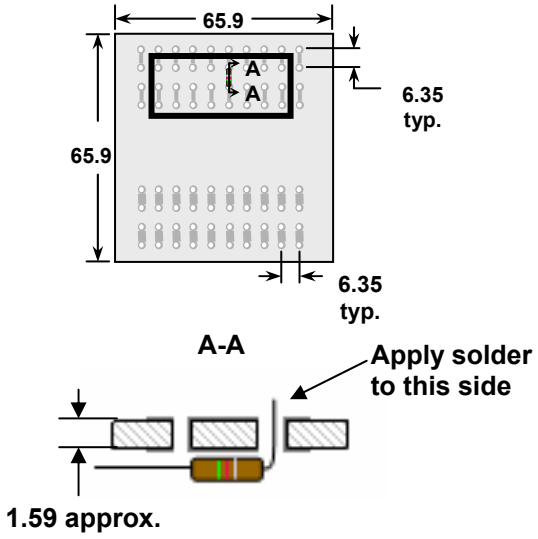

Figure 1. Plated through-hole sample configuration used during reduced gravity testing. All dimensions in millimeters.

Part way through the test series, a magnified camera view provided improved video imaging of each joint as it was soldered. The camera was a Hitachi Color Camera (model KP-C553U) and used a Nikor 105mm Macro Lens. This camera / lens combination produced a field-of-view of 5.7 mm width by 7.5 mm height at the working distance. From the video, we were able to directly observe various aspects of the soldering process including heating characteristics, flux vaporization, fillet volume evolution, bubble evolution, and solidification.

III. Experimental Observations and Results

A. Previous Results

To date, we have generated 1347 solder samples in the plated through-hole (PTH) configuration, including 938 low-gravity samples (with some partial-gravity samples) and 409 normal-gravity samples. Testing was performed during 8 flight-weeks and used seven test operators. The test matrix initially used solder (60/40 Sn/Pb) with a resin flux core. The resulting solder joints showed dramatic increases in internal porosity for joints formed in reduced gravity compared with joints made in 1-g_e[3,4], which, according to NASA standards[6], are a rejection criterion for soldered joints. Several attempts were made to minimize the amount of porosity which developed in joints formed in reduced gravity, including using solid core solder wire with either an externally applied liquid flux or a gel flux, adjusting the pre-heat and post-heat times, and de-moisturization (by an oven bake) of the circuit board itself prior to soldering. These techniques met with varying degrees of success, with the porosity results being described elsewhere[3,4,5] and in future publications. In this paper, we examine how some of these alternate soldering techniques, in addition to gravity, affect the external geometry of the solder joint.

B. Leg Length Ratios

A measure of the joint geometry is the ratio of leg lengths, L_T (top leg) to L_B (bottom leg), as shown in Figure 2. The leg lengths were measured using digitized, magnified images of the complete solder joint (prior to cross-sectioning for internal examination). The resulting mean leg length ratios for various test conditions are shown in Table 1. The measurement uncertainty for each leg is estimated to be ± 2 pixels (± 0.02 mm), unless noted otherwise. The uncertainty listed in Table 1 and subsequent tables reflects a 95% confidence interval (unless otherwise noted) on the mean value assuming a normal distribution for the leg-length ratio data set and the individual measurement uncertainties of each sample.[7] The data set consists of samples taken from all flight weeks that share the same solder / flux combination. The data in Table 1 does not differentiate between samples with different pre- and post-heating times nor does it take into account baked (i.e. de-moisturized) vs. non-baked boards. Also, we did not differentiate samples with different resistor lead diameters since the mean value of the leg-length ratio from these tests did not statistically differ from the entire dataset. With regard to acceleration, the data is grouped in sets taken in normal-gravity and nominally 0-g_e cases. In previous reports[5] we have applied a filter to remove cases where the measured acceleration showed significant g-jitter. The acceleration filters (thus g-jitter) had minimal impact on the leg-length ratio data. Consequently, the data in Table 1 is unfiltered with regard to acceleration. The data set was filtered, however, to remove joints which were biased in the following way: (1) joints which failed the NASA visual inspection due to insufficient or excess mass of solder, (2) joints where the vertical distance of the lead was insufficient to allow unimpeded growth of the solder fillet, effectively constraining the solder to a maximum leg length on one or both sides, (3) joints with very poor wetting (e.g. poor flow to the bottom leg resulting in a $L_T/L_B>5$), and (4) joints where the lead and the circuit board are not perpendicular in the imaging plane. This filter removed approximately 19% of joints that were available for analysis.

The data in Table 1 indicates that more solder flows through the plated-though-hole in normal gravity than zero-gravity. While this is intuitive, a more surprising result is that the joints formed in near 0-g_e are not perfectly symmetric. Specifically, the leg lengths are larger on the top of the joint (where the solder is added) than on the bottom. In the following sections, we present various experimental observations some of which were obtained from recent video data which may help explain this phenomenon. A discussion follows which offers some explanation of these observations.

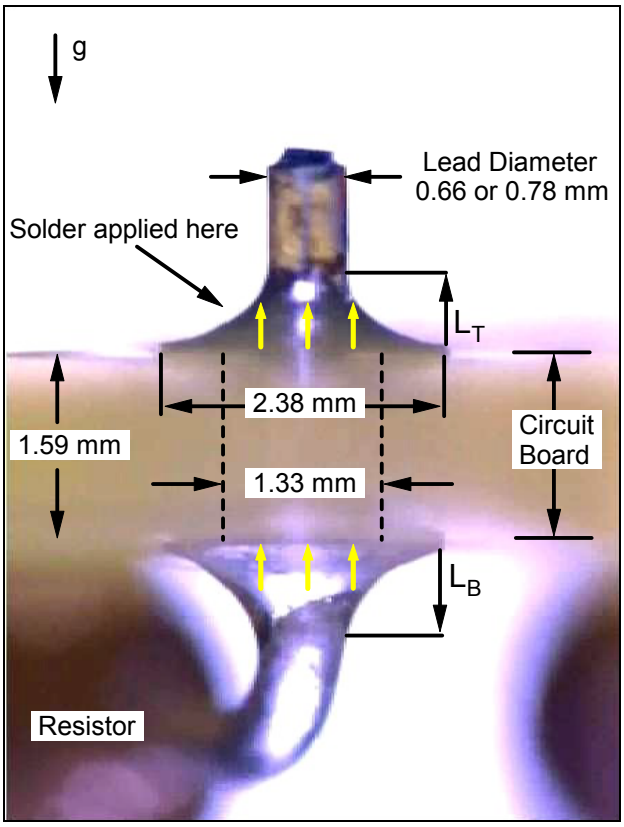

Figure 2. Image of a solder joint formed during this experiment. The yellow lines denote typical directions of solidification wave propagation discussed Section III(F).

Test condition	$1\text{-}g_E$		$0\text{-}g_E$	
	Samples	L_T/L_B	Samples	L_T/L_B
Flux Core Solder	222	0.76 ± 0.03	381	1.08 ± 0.04
Solid Core Solder & Liquid Flux	91	0.71 ± 0.10	198	1.16 ± 0.04

Table 1. Comparison of mean leg-length ratios for a given combination of flux type and acceleration level. The "Samples" column indicates the number of joints in the population for the computed mean. The uncertainty reflects a 95% confidence interval assuming a normal distribution for the leg-length ratio.

C. Heating Effects

From the perspective of repairs aboard spacecraft, controlling the quality of the joint by optimally applying heat is a logical step. From the video, we measured heating times (accurate to within 1/30 of a second) defined as follows: (a) "preheat time" is the time from when the solder iron establishes mechanical contact with the pad until solder is first added to the joint; (b) "solder addition time" is the time when solder is added to the joint inclusive of multiple additions by the operator; (c) "post-heat time" is the duration from the completion of solder addition to soldering iron removal; and (d) "solidification time" is the duration from soldering iron removal to complete solidification of the joint. Solidification was visually observed by changes in the appearance of the solder as discussed in section III.F. The validity of this method was confirmed by thermocouple data obtained from a subset of samples.

During portions of the experiment, we controlled the pre- and post-heating times. Nominally, we chose both pre- and post-heat intervals of 3 and 6 seconds which we deemed as optimal and slightly excessive, respectively. Although pre- and post-heat times were only loosely controlled, actual heating times for each test were extracted

through video analysis. Data from tests where the timing was not specifically controlled but did fall into a desired interval were included in the subsequent analysis.

First, we consider the effect of post-heat on the leg-length ratio in 0-g_e as shown in Table 2 (flux-cored solder) and Table 3 (solid core solder with liquid flux). In Tables 2 and 3, we divided the data into groups with post-heat times of less than 3 seconds and those with post-heat times of greater than (or equal to) 3 seconds. The mean value, μ, and standard deviation, σ, of these data sets are shown in each table to give a better representation of the dataset being compared. In the case of flux-cored solder (Table 2), pre-heat time was not deemed important to precisely control (i.e. no flux to vaporize) but was nominally 2.61 ± 1.80 seconds (standard deviation) for the dataset presented. In the case of solid-core solder with liquid flux (Table 3), all preheat values are included in the dataset. Table 2 shows that post-heating does not affect the leg-length ratio for flux-cored solder. For the solid-core solder with liquid flux data shown in Table 3, longer post-heat times resulted, on average, in larger leg-length ratios, though we note that the 95% confidence intervals indicate that the mean values could be similar.

Test condition	**POST-HEAT < 3 SEC.** ($\mu = 1.69$, $\sigma = 0.70$)		**POST-HEAT ≥ 3 SEC.** ($\mu = 4.21$, $\sigma = 1.42$)	
	Samples	**L_T/L_B**	**Samples**	**L_T/L_B**
Flux Core Solder (all pre-heat times)	286	1.07 ± 0.04	95	1.09 ± 0.08

Table 2. Comparison of mean leg-length ratios for flux cored solder with short and long post-heat times in a nominally 0-g_e environment.

Test condition	**POST-HEAT < 3 SEC.** ($\mu = 1.77$, $\sigma = 0.63$)		**POST-HEAT ≥ 3 SEC.** ($\mu = 4.65$, $\sigma = 1.60$)	
	Samples	**L_T/L_B**	**Samples**	**L_T/L_B**
Solid Core Solder & Liquid Flux (all pre-heat times)	109	1.10 ± 0.06	89	1.22 ± 0.06

Table 3. Comparison of mean leg-length ratios for solid core solder / liquid flux with short and long post-heat times in a nominally 0-g_e environment.

For solid-core solder and liquid flux combination, it is important to pre-heat the joint to allow the flux to clean the surface and subsequently vaporize the residual flux. Table 4 shows the effect of pre-heat time (nominally 3 and 6 seconds) on the leg - length ratio for joints soldered with solid-core wire and liquid flux. Two subsets are presented: (1) considering all solid-core solder / liquid flux cases that fall within the specified pre-heat interval irrespective of post-heat time and (2) considering only those with 3.0 ± 1.0 seconds of post-heat time. We included the latter subset to separate out the simultaneous effects of varying pre- and post- heat times. Because of limited sample numbers, we could not generate these subsets for all variable combinations. The data in Table 4 shows that the pre-heat times considered did not affect the leg-length ratio of the solder joints. The subset including only a 3.0 ± 1.0 second post-heat interval did show a larger mean leg-length ratio for the shorter pre-heat interval. This same subset, however, does have a significantly larger confidence interval, thus making that data subset statistically the same as the comparison subset.

Test condition	**3-SECOND PRE-HEAT**		**6 SECOND PRE-HEAT**	
	Samples	**L_T/L_B**	**Samples**	**L_T/L_B**
Solid Core Solder & Liquid Flux (all post-heat times)	80	1.15 ± 0.07	45	1.14 ± 0.10
Solid Core Solder & Liquid Flux (3±1 second post-heat)	25	1.25 ± 0.19	25	1.14 ± 0.13

Table 4. Comparison of average leg-length ratios for 3 and 6 second pre-heat times (± 1 second) for solid core solder / liquid flux in nominally 0-g_e environment.

Finally, we conclude this section by stating some observation regarding mechanical influence of the soldering iron on the joint shape. In most cases, the solder iron placed the resistor lead under some tension which, upon removal of the iron, caused the lead to spring back to its equilibrium position. Another observation was that some solder tended to adhere to the iron and deformed the joint shape as the iron was removed. In some cases, solder remained on the iron. These effects typically were observed to have only a momentary influence on the solder joint and recovered to the near-final joint profile within a few video frames. In some cases, however, these mechanical influences tended to persist, particularly (although not exclusively) with the solid-core solder. For example, a visible bulge caused by solder iron removal remained on the surface of the joint after solidification, as shown in Figure 3.

Figure 3. Example of a persistent effect of soldering iron removal observed on a few joints during this experiment.

D. Flux Addition and Vaporization

For test conditions involving solid solder, test-operators were directed to apply a single drop of liquid-flux on the joint prior to soldering. A typical sequence of the flux vaporization is shown in Figure 4. After application of the flux (Figure 4A) and upon the application of heat, the flux began to vaporize (Figure 4B). Generally, the flux appeared to evaporate completely on the pad. For cases where the flux spilled over the pad onto the circuit board material, however, residue material would appear around the edges of the pad on the circuit board. In many cases, this excess flux would continue to bubble but would not completely evaporate (Figure 4C) despite post-heat times of up to 6 seconds. This last observation suggests that gas is evolving from the circuit board material.

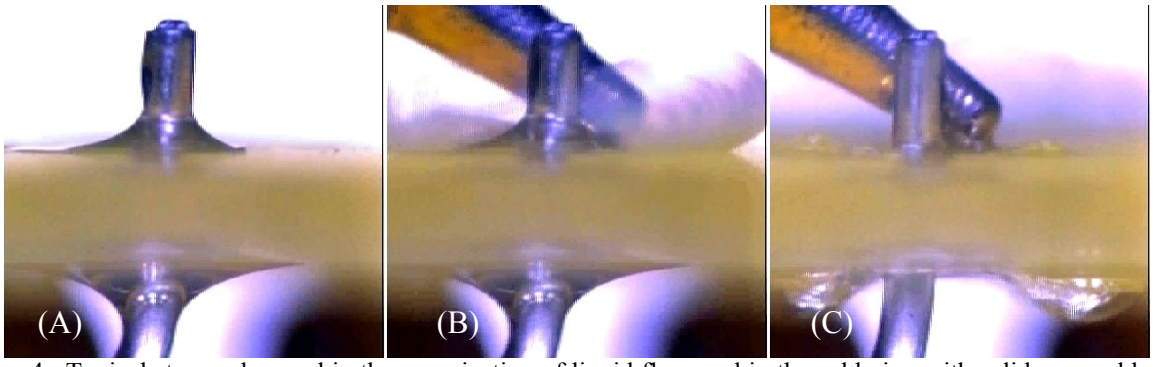

Figure 4. Typical stages observed in the vaporization of liquid flux used in the soldering with solid-core solder. A) Initial flux fillet, before heating. B) Application of heat, showing vaporizing flux. C) Flux has mostly vaporized away from joint area, but some boiling (either flux or water vapor from board) visible on bottom surface.

Using image analysis techniques discussed in the subsequent section, we measured the volume of liquid-flux added to the joints soldered with solid-core solder. For a typical subset of the normal gravity tests (43 samples), the average amount of flux added to each joint was 3.0 ± 1.2 mm^3 where the error bar is 1 standard deviation. Similarly

in 0-g_e (75 samples), the mean quantity of flux added was 3.4 ± 1.9 mm^3. For reference, the volume of the annulus between the circuit board pad and resistor lead* is approximately 1.6 mm^3 which is the minimum resolution of our measurement. An examination of possible influences of the quantity of flux added on the leg length ratio did not reveal any strong correlation.

E. Fillet Shape Evolution

Video data with images such as shown in Figures 2 provided time-resolved images of the solder fillet evolution for select joints. A custom computer program analyzed the videos in an automated fashion. The program determined the top and bottom fillet shape as a function of time (i.e. each video frame) as shown in Figure 6 where the red lines denote the fillet boundary. Both top and bottom fillet volumes were computed from the fillet profiles as volumes of revolution assuming symmetry about the resistor lead and subsequently subtracting out the volume of the resistor lead. A ± 1 pixel variation in each detected edge resulted in typical volume uncertainties of ± 0.020, 0.038, and 0.057 mm^3 for a 0.5, 1.0, and 1.5 mm^3 fillet volume (top or bottom), respectively. These values correspond to a maximum systematic error of approximately 4% in the volume measurements. Random errors associated with the measurement of the fillet profile are significantly smaller than this because of the resolution of our images (i.e.. a random uncertainty of ± 1 pixels for fillet width measurements average to near zero as measurements are made along the resistor lead).

In approximately 230 samples analyzed in this fashion, we observed two general categories of behavior. About 67% of these tests showed smooth growth of the bottom fillet, with no apparent expulsion of bubbles, whereas about 33% showed considerable disturbances from gas bubbles expanding and leaving the solder fillet. Both general types of behavior are examined in the following subsections.

1. Samples Exhibiting No Apparent Bubble Evolution

Figure 5 is a plot of the fillet volumes as a function of time for a case typical of those that did not show bubble evolution. In this plot, the colored bars on the charts correspond to events in the soldering process: the yellow region represents the time period where heat is applied to the joint via the soldering iron, the cross-hatched gray region denotes the time period where solder is applied and the blue region represents the time period after the soldering iron is removed and the solder is still molten. The left edge of the blue denotes when the soldering iron is removed and the right edge of the blue region corresponds to when the joint is completely solidified†. The fillet volume is difficult to compute on the top of the joint when the soldering iron is in contact with the solder. Consequently, the top fillet volume is not displayed until the soldering iron is removed. Additionally, the top and bottom volumes do not account for the solder in the annular region between the circuit board and the resistor lead.

An interesting feature of Figure 5 is the change in the bottom fillet volume as the soldering iron is removed. Near the end of the heating period (~ t=9.5 seconds or end of yellow region) the bottom fillet volume decreases sharply and then increases back to near the original volume. A sequence of frames from the analyzed video (Figure 6A-6C) help illustrate this. As the soldering iron is removed, the molten solder is pulled up with the iron tip and then redistributes itself quickly when the iron is completely detached from the solder. This is evident in the bottom fillet shown in Figure 6B which is clearly smaller than in either 6A or 6C. The bottom solder fillet in 6C is redistributed to nearly the same configuration as in 6A in about 0.13 seconds. In other cases, the soldering iron was removed from the solder with no apparent disturbances in the joint shape. In cases where there was minimal influence by the soldering iron and bubble evolution, the total fillet volume (top + bottom + annulus) would decrease by roughly 5% upon solidification (on average). This volume decrease was consistent across all conditions and is higher than values reported in the literature [8,9] of 3-4 % volume decreases during solidification.

2. Samples that Exhibited Bubble Evolution

The data in Figure 7 is representative of the subset of tests that exhibited bubble evolution (including 0-g_e and 1-g_e tests). This plot shows the fillet volume measurements of a sample with two types of bubble evolution: those that expand and eventually leave the molten solder and those that remain in the solder as sub-surface voids. From approximately 5.5 to 12.5 seconds, the volume measurements of the bottom fillet create a saw tooth pattern in Figure 7. This phenomenon is likely caused by bubbles that gradually expand and then quickly burst through the molten solder as shown in the sequence of images in Figure 8. In Figure 8A, a sub-surface gas bubble apparently

* Only the 0.66 mm diameter resistor lead was used for video analysis.

† Thermocouples temperature measurements from select joints correlated well with our visual determination of solidification (e.g. Figure 2 from reference 3).

begins to expand. As shown in the fillet volume plot (Figure 7) the fillet continues to expand for 1.87 seconds until it reaches its maximum volume (Figure 8B). At this point, the gas bubble is evolved and the solder rapidly contracts (Figure 8C); this is especially evident in the lower fillet. Again, note that the solder joint is redistributed quickly after the gas bubble leaves the solder.

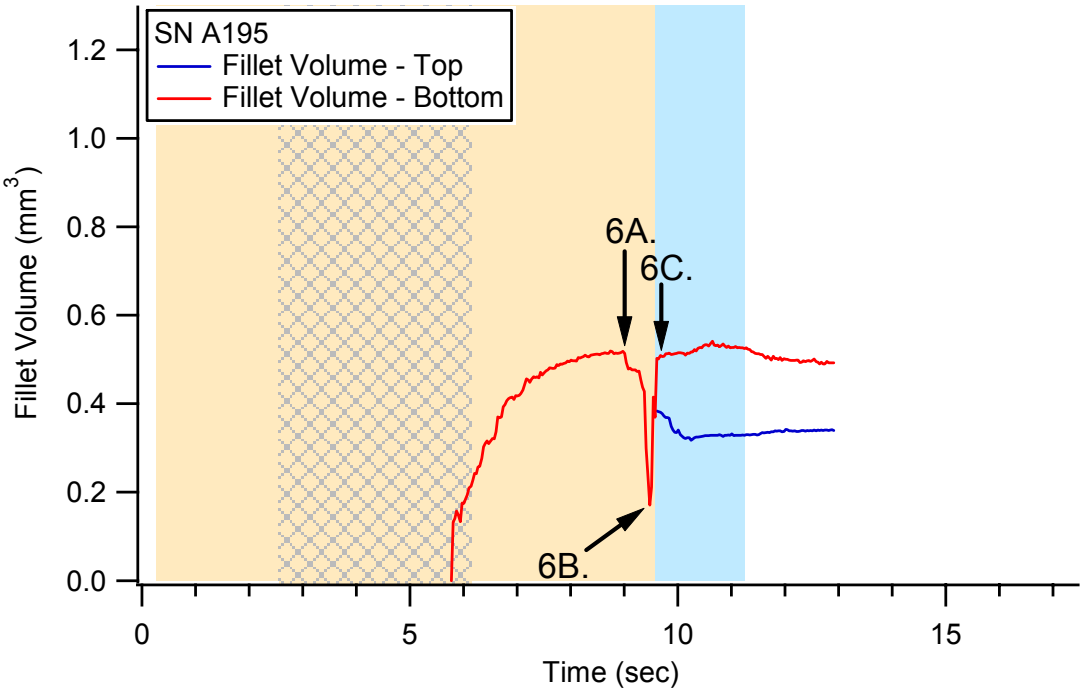

Figure 5. A fillet volume vs. time graph for a flux-cored solder joint produced in normal-g_e.

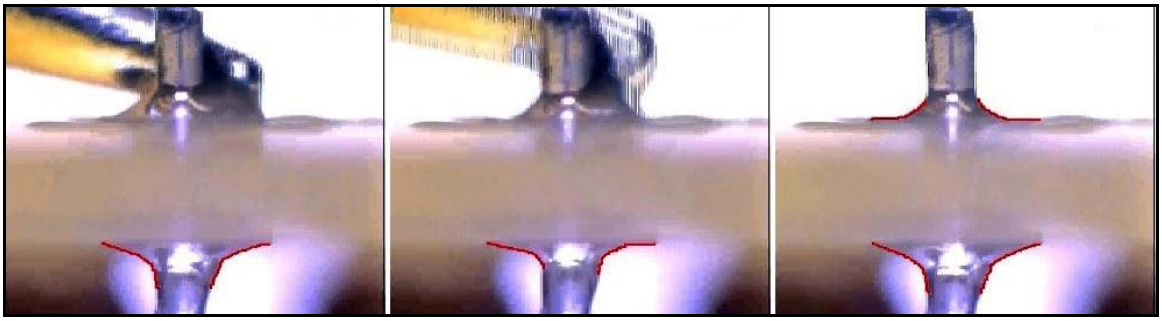

Figure 6. A sequence of frames from the analyzed video shown to demonstrate the effect of removing the soldering iron from the joint. The letters denote the corresponding volume measurements in Figure 5 where (A) = 9.33 sec. (B) =9.43 sec. (C) = 9.56 sec.

In some cases, it appears that an expanding bubble is trapped in the joint as it solidifies. This can also be seen in the top fillet volume of Figure 7 where the volume increases during the cooling period (the blue bar). Video images corresponding to these measurements are shown in Figure 9. In Figure 9A, the top left fillet appears to be concave, but expands to a convex shape 1.63 seconds later due to a sub-surface bubble in Figure 9B and subsequently solidifies.

Finally, we note the disturbance to the bottom fillet volume as the soldering iron is removed (at the interface between the yellow and blue shaded sections of the plot) in Figure 7. As was observed for the case in Figure 5, the bottom fillet responded to and recovered from the disturbance caused by the soldering iron's removal within about 1/10 of a second.

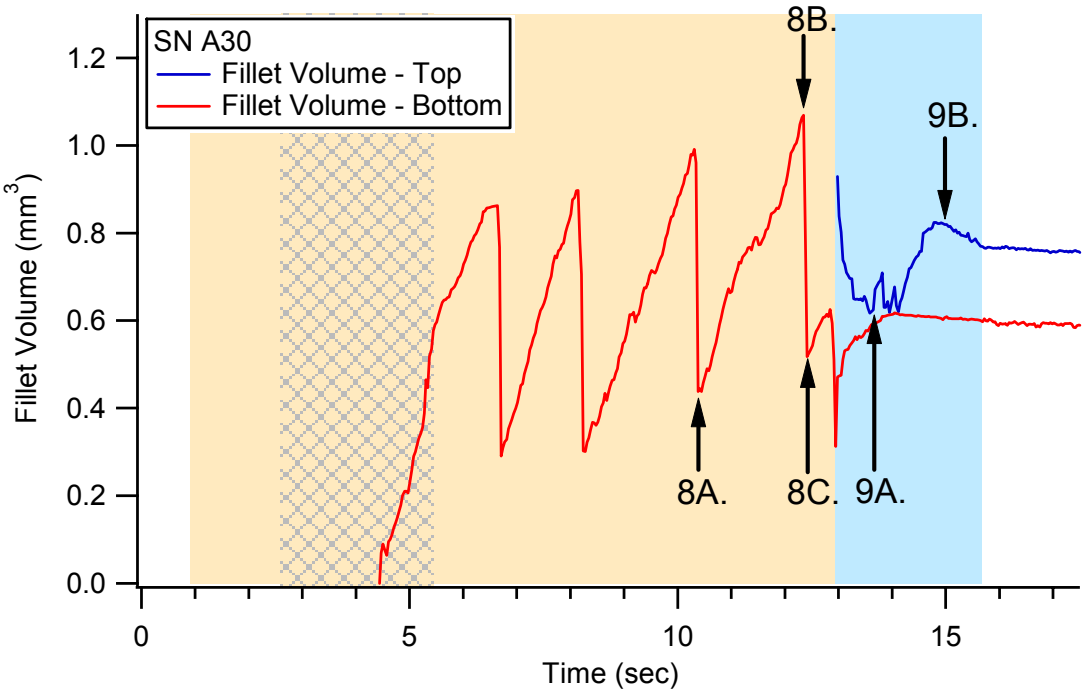

Figure 7. Fillet volume – time graph showing bubble evolution (flux-cored solder in 0.38-g_e or Martian gravity). Frames from corresponding images (Figure 8 and 9 below) are denoted in the graph.

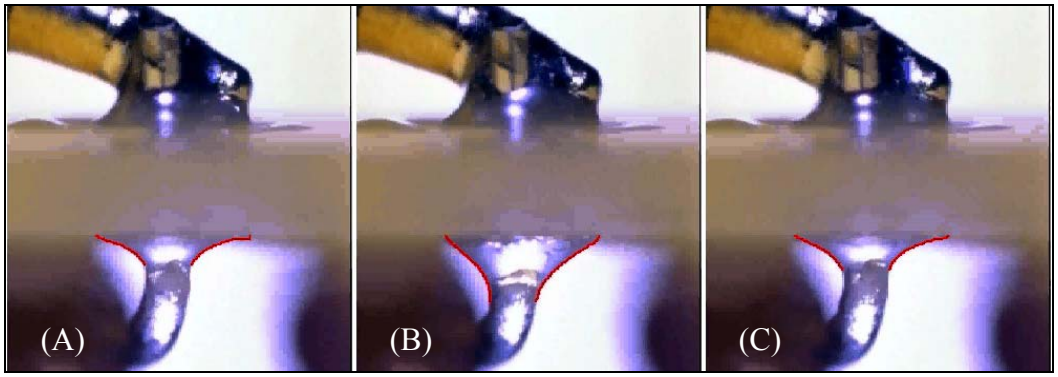

Figure 8. A sequence of frames from the analyzed video demonstrating a bubble evolving from the joint. The letters denote the corresponding volume measurements in Figure 7 where (A) = 10.43 sec. (B) = 12.30 sec. (C) = 12.36 sec.

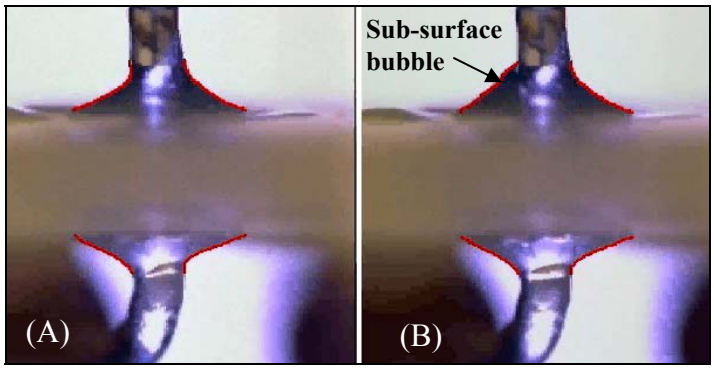

Figure 9. A sequence of frames from the analyzed video demonstrating a sub-surface bubble expanding the top fillet volume but solidifying prior to escaping the joint. The letters denote the corresponding volume measurements in Figure 7 where (A) = 13.43 sec. and (B) = 15.06 sec.

F. Solidification

Joint solidification was visible (or partially visible) in the video analysis on many but not all joints. In a large majority of the cases, 2 separate solidification waves would be seen propagating across the joint as shown by the yellow arrows in Figure 2. For the upper half of the joint, the solidification front would begin typically near the circuit board and propagate up toward the exposed lead. It is important to state that this was observed in the majority of the cases but not all. Reverse trends where the solder started solidifying at the top were occasionally seen (~15% of the analyzed joint) for the upper joint. In a few cases, solidification waves were observed on both the top and bottom of the upper joint, meeting approximately in the middle (~1%). On the lower joint, the solidification wave primarily began at the bottom of the joint (near the exposed lead) and progressed towards the circuit board. Similar to the upper joint, we observed both the reverse trend and occasional dual waves on the bottom. A wave required roughly 1 second to propagate across either the upper or lower joint. Finally, about 60% of the joints finished solidifying on the upper joint prior to completion of solidification on the lower joint. The above observations spanned the entire dataset regardless of gravity, solder / flux combination, and pre- and post-heating times. Initial correlations of these observations with experimental variables were inconclusive.

G. Circuit Board Moisture

In the literature, we found research that attributes joint porosity to both entrapped flux[8] and water vapor[10]. The water vapor apparently is absorbed by the laminate material of the circuit board. As the joint is heated, the water vapor evaporates and escapes as steam through small cracks in the circuit board and metal pad. This gas then can be entrapped in the joint as it solidifies causing joint porosity. While porosity is the topic of another paper, we also examined the effect of circuit board moisture on the leg length ratio. To remove any entrapped circuit board moisture, we baked a select number of boards at 200°F for at least 4 hours and subsequently kept the boards in a dry environment until soldering.

Test condition	$1\text{-}g_E$		$0\text{-}g_E$	
	Samples	L_T/L_B	Samples	L_T/L_B
Flux Core Solder / Non-Baked Boards	176	0.79 ± 0.04	251	1.11 ± 0.04
Flux Core Solder / Baked Boards	46	0.63 ± 0.05	130	1.01 ± 0.08
Solid Core Solder & Liquid Flux / Non-Baked Boards	87	0.70 ± 0.10	178	1.13 ± 0.05
Solid Core Solder & Liquid Flux / Baked Boards	4	N/A	20	1.38 ± 0.14

Table 5. Comparison of average leg-length ratios for tests with boards that were oven-baked to remove moisture to those not baked prior to soldering.

The flux-core solder data in Table 5 shows that joints formed in $0\text{-}g_e$, on average, had a leg length ratio slightly closer to unity for cases that were baked compared with joints that were not baked. Confidence interval calculations show that while the distributions overlap at the 95% confidence interval, they can be considered statistically different at about a 90% confidence level. Results for flux-core, baked boards in normal gravity show significantly smaller L_T/L_B ratios than the non-baked case. The solid-core solder data in Table 5 showed opposite behavior namely that joints formed in $0\text{-}g_e$ on baked boards had significantly higher leg-length ratios than those that were not baked. Despite the relatively few samples of the baked boards with solid-core soldered joints, the confidence intervals suggest that this is a statistically valid observation. We did not have a statistically significant number of samples in normal gravity for the baked boards with solid-core soldered joints.

H. Mass of Solder Added

On average, solid-core solder joints received more mass than flux-cored joints (Table 6). Also, operators tended to add slightly more solder, on average, in the reduced gravity tests than in the normal gravity tests. This is an interesting observation in that operators were required only to add (what they deemed) an optimal amount of mass to the joint*. We measured solder mass by using pre-cut solder pieces which were weighed before and after the tests. Table 6 shows the average solder mass added (and standard deviations of the dataset) in both normal and reduced gravity for all test operators, for both flux core solder and solid solder. The 95% confidence intervals for the mean values listed in Table 6 were approximately ± 1 mg for each sample population.

* All test operators received standardized training in PTH soldering.

Test condition	1-g_E		0-g_E	
	Samples	Mass (g)	Samples	Mass (g)
Flux Core Solder	240	0.026 ± 0.006	440	0.028 ± 0.009
Solid Core Solder	158	0.033 ± 0.009	369	0.035 ± 0.011

Table 6. Mean solder mass added for all tests grouped by acceleration level and soldering condition. The error bars denote one standard deviation of the dataset.

IV. Discussion

We begin the discussion by stressing that the data presented has sample populations that are large enough to make statistically valid observations for each condition. This fact is important in solder leg-length measurements (and other parameters) where we observed differences from joint to joint. There were cases which significantly differed from the mean values reported or even were opposite the general trends. Factors such as surface roughness, joint preparation, and solder iron handling are just some factors which can affect fillet formations. Not all these factors can be precisely controlled but this is the case in almost any practical repair environment.

The data presented shows that PTH solder joints form asymmetrically, on-average, in both normal and reduced gravity. In normal gravity (as shown in Table 1), larger leg-lengths are observed below the circuit board compared to above the circuit board. In reduced gravity, the reverse trend is observed, namely, larger leg-lengths are observed above the circuit card than below, though we note that the reduced gravity values are closer to unity than the normal gravity values. One possible explanation is that the smaller driving potential caused by the reduction in the (gravitational) body force slows the transport of solder from the top to bottom of the joint, and therefore the joint does not have sufficient time to reach its ideal equilibrium shape (i.e. $L_T/L_B = 1$) prior to joint solidification. While the tendency of the L_T/L_B to exceed unity in the reduced gravity case would seem to support this, closer examination of the data suggests that this simple explanation may be insufficient. Many tests, both in normal and reduced gravity, showed that the fillet geometry responded fairly quickly to disturbances such as the removal of the soldering iron. These tests demonstrated that fillet volumes (and by extension, leg lengths) tended to re-acquire their 'pre-disturbance' values within tenths of a second after the disturbance. This fast response time to external disturbance suggests that surface tension forces alone can cause the fillet to achieve its equilibrium shape quickly and independent of body forces.

A possible explanation of the behavior of the L_T/L_B ratio may be in terms of the initial fillet growth, rather than fillet response time. For a majority of the normal gravity cases, the bottom fillet appeared to reach its near final shape almost immediately after solder addition was complete. Cases with smaller amounts of mass added (such as Figure 5), however, appeared to take a few seconds to equilibrate after all of the solder was added to the joint. In reduced gravity, the initial formation of the bottom fillet appeared to evolve more slowly for several cases including some which increased up until soldering iron removal. Upon closer examination of these tests, however, it appeared that non-gravitational effects could account for the slower bottom fillet evolution for some cases. For example, the application of the solder was not a steady process from test to test – operators would occasionally apply the solder in several discrete intervals. Also, the location of solder application varied somewhat from cases to case including directly to the pad, resistor lead, or on the solder iron. All these effects appeared to play some role in the initial evolution the solder fillet.

After the solder addition was complete, we observed several cases where the bottom volume appeared to increase for a considerable time (in some cases up to soldering iron removal). Some of these cases appeared to be explained by bubble evolution or other non-gravitational effects. In one interesting case, we observed a joint that initially looked like Figure 3 after solder iron removal. The solder "spike" was slowly absorbed by the joint and eventually reached a more typical shape although it required several seconds to equilibrate – this slow transition manifested itself as a slow change on the bottom fillet volume evolution plot. Nonetheless, it must be said that there were some select cases which support the notion that solder fillet growth is influenced by gravity. To this end, we have not taken into account any g-jitter effects which, although they did not affect the average leg-length ratio, may influence fillet evolution depending on its severity. Therefore, we can only conclude that the fillet evolution is a complex process that can be affected by many factors including gravity, solder mass added, solder application technique, joint preparation, etc.

We controlled both pre- and post-heat times for many of the solder joints formed. While the primary purpose of this was to investigate its effect on joint porosity, we did look at how pre- and post-heat times affected joint geometry. With regard to pre-heating times for activating the liquid flux prior to application of solid-core solder, we

did not see any statistically valid conclusions, as seen in Table 4. It is likely, however, that more extreme variations of pre-heat time could influence the wetting characteristics of the solder and ultimately affect joint geometry.

Considering the notion that the 'driving potential' for fillet evolution is slowed in the reduced gravity, it may seem that merely applying longer post-heat would give the system more time to equilibrate, and should leave more geometrically uniform joints. The data, however, does not support this idea. Examination of Tables 2 and 3 shows that for both flux core solder and for solid solder with liquid flux, increasing the post-heat time does not drive the L_T/L_B ratio closer to unity.

We believe that the reason that post-heat time does not affect joint geometry is that the soldering iron itself distorts the joint, by providing a relatively large area on the top fillet for the solder to adhere to. While small amounts of flow (i.e. bottom fillet evolution) do occur during the post heat phase, the "settling" time in which the joint would approach its final equilibrium shape would then not truly commence until the iron is removed. Examination of Figures 5 and 7 in the beginning of the blue shaded region shows that the bottom fillet tends to grow slightly after the iron is removed. However, this slight growth can be offset by the natural shrinkage of the solder fillet as it cools. In fact, there were many cases (not shown) in which both top and bottom fillet volumes immediately began to shrink upon removal of the soldering iron.

The period between soldering iron removal and complete joint solidification is perhaps the best region to determine whether or not there is sufficient time or driving force for the joint to hydrodynamically stabilize at L_T/L_B =1 prior to solidification. Examination of all of the available data is somewhat inconclusive. While some cases showed that the bottom fillet grew while the top fillet decreased in volume, the overwhelming majority of top and bottom fillets tended to both shrink during this cooling period. This suggests that the solidification occurs rapidly inside the joint, suppressing any observable flow. The joint may be freezing in the annular region (where the ratio of surface area to volume is quite high), thereby stopping hydrodynamic communication between the top and bottom fillets early in the cooling process. If in fact mass transport from top to bottom is slower in reduced gravity, annular solidification could explain why we see leg-length ratios greater than unity in 0-g_e. The solidification observations presented, however, cannot be interpreted easily to explain the solidification in the annular region.

Another potential reason for larger L_T/L_B ratios in 0-g_e may be inferred by examination of Table 5. The data for flux-cored solder shows that joints produced with baked circuit boards have L_T/L_B ratios much nearer to unity than joints formed on non-baked boards. Also, as we described earlier, bubble evolution was more prevalent on joints formed on non-baked boards. It is conceivable that bubbles evolving in the annulus region of the solder joint could act as an obstruction to solder flow from top to bottom of the circuit card. It is emphasized, however, that the exact opposite behavior occurred, namely even larger L_T/L_B ratios, using solid-core solder with liquid flux on baked circuit cards. Further examination, perhaps with a detailed look at each joint's porosity, may help explain this observation.

A final observation regarding joint shape comes from comparing the amount of mass added to the joint using flux-cored vs. solid-core solder (Table 6). This data shows almost a 35% increase in the mass added to the joint when using solid-core solder compared to flux-core. This effect was observed both in normal and reduced gravity although operators tended to add slightly more solder in reduced gravity. A simple explanation could be that the feed wire diameters were larger for the solid-core wire (0.79 mm OD) compared with the flux-cored wire (0.64 mm OD), meaning that the solid-core wire has greater volume per unit length of feed wire.

Another possible explanation regarding the increase in mass added from flux-core to solid-core solder could be differences in wettability between the two solder types. This could be caused by small variations in flux applications, which could lead to non-wetting of the resistor lead. In the flux-cored case, the continual presence of flux ensured good wetting. These variations may have caused operators to add more solder in the cases where poor initial wetting occurred. While these observations could explain the differences of mass added between flux and solid-core solder, the subtle variations in mass between reduced and normal gravity may be complex and are not easily explained.

Taken together, these observations suggest to us that the original hypothesis of inadequate time or driving force for the joint to equilibrate before solidification may still be valid. The transport of mass from the top to bottom of the joint begins when sufficient mass is added to wet the top of the joint and concludes when the annulus region is solidified. Equilibration to the joints final shape, which can be confounded by bubble evolution, begins when the soldering iron is removed and ends when the joint is completely solidified. This explanation can account for the differences in leg length ratio seen in reduced gravity versus normal gravity, keeping in mind that there are other factors which appear to influence the fillet's final shape including solder mass added, solder application technique, joint preparation, etc.

V. Conclusions

In conclusion, we have demonstrated that geometrical differences exist in solder joints produced in reduced gravity, as compared to those formed in normal gravity. While normal gravity joints (formed under the influence of surface tension forces and body forces) tend to have leg-length ratios significantly less than unity, the same ratio for reduced gravity joints (subjected only to surface tension forces) tend to slightly exceed unity. These tests were carried out with both flux cored solder, and with solid solder along with liquid flux. The trends held similarly for both cases, and also seemed fairly insensitive to changes in pre-heat or post-heat times. Volume measurements made from video analysis of the joint formation shows the presence (in many cases) of significant bubble evolution, which can either directly or indirectly affect the final joint geometry. The data supports the hypotheses that reduction in the effective gravitational body force slows the transport of solder from the top to bottom of the joint preventing the joint to reach its ideal equilibrium shape (i.e. $L_T/L_B = 1$) prior to joint solidification. Transport may also be slowed by entrapped gas bubbles. We acknowledge that there are factors other than gravity which may influence the fillet's final shape including solder mass added, solder application technique, joint preparation, etc.

VI. References

[1] Winter, C. and Jones, J.C., the Microgravity Research Experiments (MICREX) Database, NASA TM-108523 (1996).

[2] ASTM Committee E-4.2001, Standard Practice for Determining the Inclusion or Secondary Phase Constituent Content of Metals by Automatic Image Analysis, Annual Book of ASTM Standards 2001, Sect. 3, Vol 03.01.(2001).

[3] Pettegrew, R.D., Struk, P.M., Watson, J.K., and Haylett, D.R., Experimental Methods in Reduced-Gravity Soldering Research, NASA TM-2002-211993 (2002).

[4] Pettegrew, R.D., Struk, P.M., Watson, J.K., Haylett, D.R., and Downs, R.S., Gravitational Effects on Solder Joints, AWS Welding Journal, pp. 44-48, October 2003.

[5] Struk, P.M., Pettegrew, R.D., Downs, R.S., and Watson, J.K., The Effects of an Unsteady Reduced Gravity Environment on the Soldering Process, AIAA-2004-1311 and NASA TM-2004-212946 (2004).

[6] Soldered Electrical Connections, NASA Technical Standard NASA-STD-8739.3 w/Change 2 (1997).

[7] Moffat, R.J., Describing the Uncertainties in Experimental Results, *Experimental Thermal and Fluid Science*, Vol. 1. pp. 3-17 (1988).

[8] Banks, D.R., Burnette, T.E., Cho, Y.C., DeMarco, W.T., and Mawer, A.J., The Effects of Solder Joint Voiding on Plastic Ball Grid Array Reliability, Surface Mount International (SMI) Proceedings, pp. 121-126 (1996).

[9] Humpston, G., and Jacobson, D.M., Principles of Soldering and Brazing, ASM International, Materials Park, OH, pp. 127-128 (1993).

[10] Lea, C., The Harmfulness of Blowholes in PTH Soldered Assemblies, *Circuit World*, Vol. 16, Issue 4 (1990).

REPORT DOCUMENTATION PAGE

Form Approved
OMB No. 0704-0188

1. AGENCY USE ONLY (*Leave blank*)	2. REPORT DATE	3. REPORT TYPE AND DATES COVERED
	May 2005	Technical Memorandum

4. TITLE AND SUBTITLE

The Influence of Gravity on Joint Shape for Through-Hole Soldering

5. FUNDING NUMBERS

WBS–22–101–42–02

6. AUTHOR(S)

Peter M. Struk, Richard D. Pettegrew, Robert S. Downs, and J. Kevin Watson

7. PERFORMING ORGANIZATION NAME(S) AND ADDRESS(ES)

National Aeronautics and Space Administration
John H. Glenn Research Center at Lewis Field
Cleveland, Ohio 44135–3191

8. PERFORMING ORGANIZATION REPORT NUMBER

E–15057

9. SPONSORING/MONITORING AGENCY NAME(S) AND ADDRESS(ES)

National Aeronautics and Space Administration
Washington, DC 20546–0001

10. SPONSORING/MONITORING AGENCY REPORT NUMBER

NASA TM—2005-213589
AIAA–2005–0541

11. SUPPLEMENTARY NOTES

Prepared for the 43rd Aerospace Sciences Meeting and Exhibit sponsored by the American Institute of Aeronautics and Astronautics, Reno, Nevada, January 10–13, 2005. Peter M. Struk, NASA Glenn Research Center; Richard D. Pettegrew and Robert S. Downs, National Center for Space Exploration Research, Cleveland, Ohio 44135; and J. Kevin Watson, NASA Johnson Space Center. Responsible person, Peter M. Struk, organization code RUC, 216–433–5948.

12a. DISTRIBUTION/AVAILABILITY STATEMENT

Unclassified - Unlimited
Subject Categories: 16, 26, and 29

Available electronically at http://gltrs.grc.nasa.gov

This publication is available from the NASA Center for AeroSpace Information, 301–621–0390.

12b. DISTRIBUTION CODE

13. ABSTRACT ***(Maximum 200 words)***

An ongoing research effort on reduced gravity soldering is being conducted jointly by the National Center for Space Exploration Research, the NASA Glenn Research Center, and the NASA Johnson Space Center. Significant changes in porosity and geometry of plated through-hole (PTH) solder joints are observed in reduced gravity as compared to normal gravity. With regards to geometry, experimental data indicates that through-hole solder joints form asymmetrically in both normal and reduced gravity with respect to the amount of solder on either side of the circuit board. In normal gravity, more solder material is observed below the circuit board compared to the amount above the circuit board where the solder is first added. In reduced gravity, the reverse trend is observed, namely, more solder remains above the circuit card than below. To help understand these results, a new and more magnified view of the joint was incorporated in the experiment (part-way through the testing) which provided both spatially and temporally resolved images of the fillet evolution and solidification during the soldering process. Results from these tests support the hypothesis that there is inadequate time or driving force in reduced gravity for the solder joint mass to equilibrate to complete symmetry from top to bottom before solidification. Equilibration to the joint's final shape, which can be confounded by bubble evolution within the joint, appears to be influenced by factors in addition to gravity such as solder mass added, solder application technique, the soldering iron, and joint preparation.

14. SUBJECT TERMS

Microgravity applications; Microgravity; Soldered joints; Soldering

15. NUMBER OF PAGES

19

16. PRICE CODE

17. SECURITY CLASSIFICATION OF REPORT	18. SECURITY CLASSIFICATION OF THIS PAGE	19. SECURITY CLASSIFICATION OF ABSTRACT	20. LIMITATION OF ABSTRACT
Unclassified	Unclassified	Unclassified	